ANTIMICROBIAL AGENTS AND CHEMOTHERAPY, Sept. 2009, p. 3985–3988 Vol. 53, No. 9
0066-4804/09/$08.00+0 doi:10.1128/AAC.00009-09

In Vitro Trafficking and Efficacy of Core-Shell Nanostructures for Treating Intracellular *Salmonella* Infections▽

A. Ranjan,[1] N. Pothayee,[2] M. N. Seleem,[3] N. Sriranganathan,[4]* R. Kasimanickam,[1] M. Makris,[4] and J. S. Riffle[2]

Department of Large Animal Clinical Sciences,[1] Macromolecules and Interfaces Institute,[2] Institute for Critical Technology and Applied Science,[3] and Department of Biomedical Sciences and Pathobiology,[4] Virginia Polytechnic Institute and State University, Blacksburg, Virginia

Received 4 January 2009/Returned for modification 31 May 2009/Accepted 6 July 2009

Nanostructures encapsulating gentamicin and having either amphiphilic (N1) or hydrophilic (N2) surfaces were designed. Flow cytometry and confocal microscopy studies demonstrated a higher rate of uptake for amphiphilic surfaces. A majority of N1 were localized in the cytoplasm, whereas N2 colocalized with the endosomes/lysosomes. Colocalization was not observed between nanostructures and intracellular *Salmonella* bacteria. However, significant in vitro reductions in bacterial counts (0.44 $\log_{10}$) were observed after incubation with N1, suggesting that the surface property of the nanostructure influences intracellular bacterial clearance.

Intracellular pathogens like *Salmonella* have developed various mechanisms to evade host defenses, and they can establish chronic infections. Aminoglycosides comprise a group of antibiotics that exhibit antimicrobial activity against gram-positive and gram-negative intracellular bacteria. The antimicrobial activities of aminoglycosides are concentration dependent (3). In spite of their efficacy against pathogens in vitro, clinical uses of aminoglycosides are limited by their inability to transport through cell membranes and reduced intracellular drug accumulation, leading to poor bacterial clearance. In addition, repeated administration of aminoglycosides can lead to drug-induced ototoxicity and nephrotoxicity (5, 11). Therefore, the intracellular clearance of *Salmonella*, mainly in macrophages, requires novel therapeutic strategies. In this regard, liposomal and polymeric nanocarriers have been investigated (4, 7). Encapsulating drugs within nanoparticles has the potential to reduce toxicity by providing slow, sustained release and to enhance delivery to the intracellular compartments where the bacteria reside. To improve the transport of antimicrobials into macrophages, it is important that the mechanism(s) of uptake and fate(s) of nanoparticle drug carriers inside the cells be understood.

Pluronic triblock copolymers comprised of poly(ethylene oxide) (PEO) terminal blocks with a poly(propylene oxide) (PPO) central block (i.e., PEO-*b*-PPO-*b*-PEO) are currently being evaluated for chemotherapy of multidrug-resistant tumors (2). The PPO segments are more hydrophobic than the water-soluble PEO blocks, and this results in increased incorporation into cells. In this study, we designed and synthesized core-shell nanostructures with PEO-*b*-PPO-*b*-PEO shells, as described previously (15), and cores containing gentamicin complexed with polyacrylate anions (PAA). A solution of fluorescein-gentamicin (1 ml, 8.8 mg gentamicin) was added to 4 ml of gentamicin sulfate solution (10 mg ml^{-1} gentamicin sulfate, 30 mg gentamicin, $\sim 3.5 \times 10^{-4}$ eq of cations) to prepare the labeled drug mixture for incorporation into the nanostructures. To fabricate the nanostructured complexes, a hydrophilic PAA-$^{+}$Na homopolymer and amphiphilic PEO-*b*-PAA-$^{+}$Na or PAA-$^{+}$Na-*b*-PEO-*b*-PPO-*b*-PEO-*b*-PAA-$^{+}$Na were codissolved in deionized water, and then fluorescein- or rhodamine-gentamicin–gentamicin sulfate solution was added dropwise to the homopolymer/copolymer solution to form a final one-to-one ratio of anions to cations in a manner reported before (9). The nomenclature describing the amphiphilic and hydrophilic nanostructures adopted for this paper is N1 and N2, respectively (N1F is labeled with fluorescein and N1R with rhodamine, and likewise for N2).

To study the uptake of nanostructures by using flow cytometry, cultured J774A.1 murine macrophage cells (10) at 80 to 90% confluence were gently scraped, seeded at 1×10^6 cells/well onto 12-well plates, allowed to attach for 48 h, and later coincubated with N1F or N2F for 1 h or 4 h in a 5% CO_2 atmosphere at 37°C. The cells were washed twice with phosphate-buffered saline to remove any nonphagocytosed nanostructures. The fluorescence intensity of each sample was analyzed by fluorescence-activated cell sorter flow cytometry (BD FACS Aria) with an excitation wavelength of 488 nm and analyzed with a 530/30-nm emission filter. For confocal microscopic examinations, J774A.1 cells seeded at 1×10^5 cells/well into the 10-mm-diameter microwells of 35-mm petri dishes (Mat-tek Corporation, United States) were incubated with N1F or N2F (100 μg/well) for 2 h or 4 h at 37°C in a humidified 5% CO_2 atmosphere. To study colocalization, an image-iT live lysosomal and nuclear labeling kit (Invitrogen, United States) was used to stain the lysosome/endosome and nuclear compartments of the cells according to manufacturer's recommendations. The wells were examined using a 63× oil-immersion objective on a Zeiss LSM 510 META confocal microscope.

Finally, a treatment efficacy study was performed by infect-

* Corresponding author. Mailing address: Department of Biomedical Sciences and Pathobiology, Virginia Polytechnic Institute and State University, 1410 Prices Pork Road, Blacksburg, VA 24061-0342. Phone: (540) 231-7171. Fax: (540) 231-3426. E-mail: nathans@vt.edu.
▽ Published ahead of print on 13 July 2009.

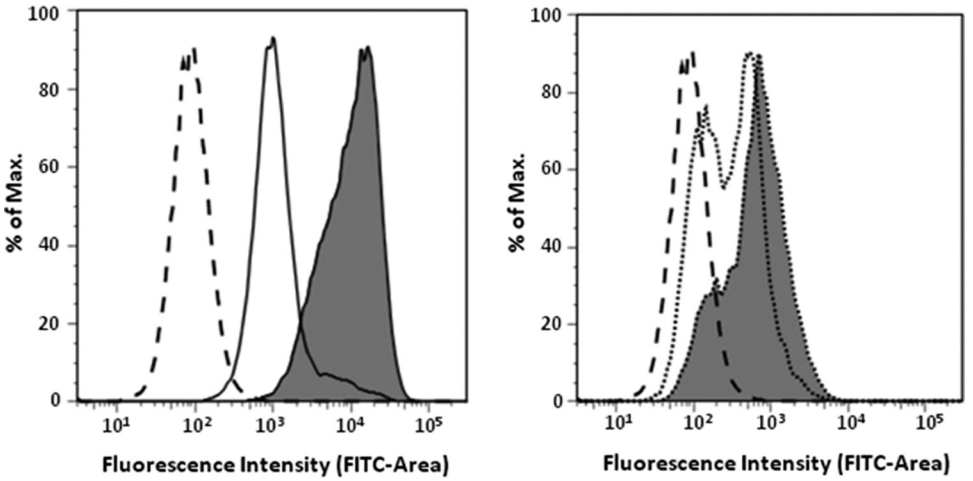

FIG. 1. Fluorescence histogram from flow cytometry depicting the uptake of nanostructures labeled with fluorescein isothiocyanate (FITC) into J774A.1 cells. Left histogram shows uptake of N1F: cells without nanostructures (dashed line), uptake after incubation with N1F for 1 h (solid line without shading), and uptake after incubation with N1F for 4 h (solid line with shading). Right histogram shows uptake of N2F: cells without nanostructures (dashed line), uptake after incubation with N2F for 1 h (dotted line without shading), and uptake after incubation with N2F for 4 h (dotted line with shading).

ing J774A.1 macrophage cells with *Salmonella enterica* serovar Typhimurium expressing green fluorescent protein (13) at a multiplicity of infection of 1:20. The infected cells were treated with 15 μg of gentamicin in solution (free gentamicin) or N1R or N2R complexes (each containing ~15 μg of gentamicin) for 4 h, and then the numbers of CFU were measured. Prior to this, the drug-releasing characteristics of the nanostructures were evaluated according to previously published procedures (9, 14, 15). In addition, infected macrophages treated with the nanostructures for 2 h were imaged by confocal microscopy to visualize any colocalization of bacteria with nanostructures. Statistical analysis was performed between groups with Student's *t* tests. The statistical significance level for the experiments was defined as a P value of <0.05.

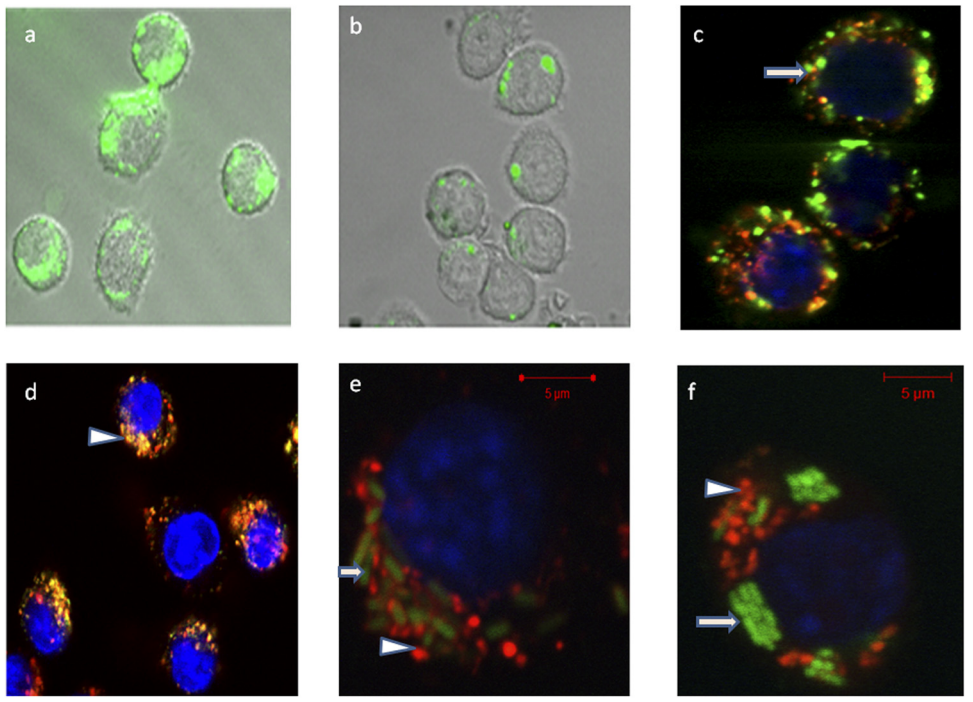

FIG. 2. Confocal microscopy. (a and b) Uptake of N2F (a) and N1F (b) nanostructures into J774A.1 cells. (c and d) Colocalization of nanostructures with endosome/lysosome after incubation for 2 h. Subcellular colocalization of N1F (arrow) (c) and N2F (arrowhead) (d) nanostructures is shown by yellow-to-orange spots formed by green nanoparticles and red endosomes/lysosomes, showing that a majority of the N2F hydrophilic nanostructures appear to reside in endosomes. (f and e) *Salmonella* (arrow)-infected J774A.1 macrophage cells incubated for 4 h with N1R and N2R nanostructures (arrowheads).

TABLE 1. Drug delivery efficacy of nanoplexes in comparison to that of appropriate controls

Group	Mean CFU ± SD	Log CFU reduction
Control	7.68 ± 0.07	0
Free gentamicin	7.70 ± 0.19	0.02[b]
N1R[a]	7.24 ± 0.03	0.44
N2R	7.67 ± 0.08	0.01

[a] Significant at $P < 0.05$.
[b] Log reduction is 0.02 times higher than the control.

Our results show that the surface chemistry of the nanostructures influences the cell uptake. Flow cytometry conducted after coincubation of J774A.1 cells for 1 and 4 h with either N1 or N2 demonstrated a higher rate of uptake for N1 (Fig. 1). This may be attributable to the increased hydrophobic character of the N1 surfaces that promote positive interactions with lipophilic cell membranes. In addition, the data are consistent with previous observations wherein the effect of block copolymers comprised of PEO and PPO was fundamentally dependent on the relative hydrophobicity (1). Greater potency of such copolymers in mediating multidrug resistance in cancer cells through interactions with the cell membranes was observed at intermediate hydrophobic PPO and relatively short hydrophilic PEO segment lengths. Interestingly, after 2 h of incubation of N1F and N2F with J774A.1 cells, confocal micrographs indicated that the cells had taken up significantly more N1F than N2F nanostructures (Fig. 2a and b). Thus, our current findings that nanostructures with PEO-PPO block copolymer surfaces (N1) enter cells more rapidly than the N2 structures having only the PEO hydrophilic surfaces seem plausible. Also, a majority of the hydrophilic N2F nanostructures appeared to reside in endosomes (Fig. 2c). In contrast, the majority of the N1F nanostructures, with amphiphilic surfaces, were found in the cell cytoplasm (Fig. 2d), suggesting that these particles may have been taken up by a different mechanism. To our knowledge, this is the first report that the hydrophilic/hydrophobic nature of aminoglycoside drug delivery vehicles can make a distinct difference in intracellular localization.

On assessment of the relative effectiveness of drug delivery, significant reductions in bacterial counts were observed with the N1 structures (0.44 $\log_{10}$) but not with N2 compared to the results for free gentamicin and infected control cells (Table 1). These results suggest that delivery of the N1 nanostructures into the cell cytoplasm has a positive effect on reducing the intracellular bacterial population. It is noteworthy that the release of gentamicin from the nanostructures at the physiological pH of 7.4 was relatively slow and sustained (Fig. 3). However, the release profiles from both nanostructures were similar, signifying that the more-hydrophobic N1 did not appreciably inhibit the release rate relative to the release rate of the more-hydrophilic N2 nanostructures. Also, coincubation of N1R or N2R with green fluorescent protein-expressing *Salmonella*-infected J774A.1 cells could not distinguish significant colocalization of bacteria and nanostructures in the confocal micrographs under these conditions (Fig. 2e and f). Longer-term incubation experiments may shed more light on this phenomenon since *Salmonella* cells escape intermittently from the host cell over extended periods and could possibly interact directly with the nanostructures in different locations during this process (12). Thus, the enhanced activity of N1 may be due either to higher bioactivity of the drug in the cell cytoplasm or increased intracytoplasmic gentamicin concentration and distribution due to greater nanostructure uptake by the macrophage cells. This is supported by the results of previous studies wherein gentamicin delivery into cells by hydrophobic microspheres correlates directly with intracellular bacterial killing (6, 8). In summary, our studies show that gentamicin encapsulation in nanostructures having amphiphilic surfaces enhances the rate and modulates the route of uptake into macrophages. This phenomenon may augment the therapeutic activity of cell-impermeable antimicrobials against intracellular bacteria.

We are grateful for NSF grant DMR-0312046 and to Virginia Tech's Institute for Critical and Applied Technologies (ICTAS) for funding.

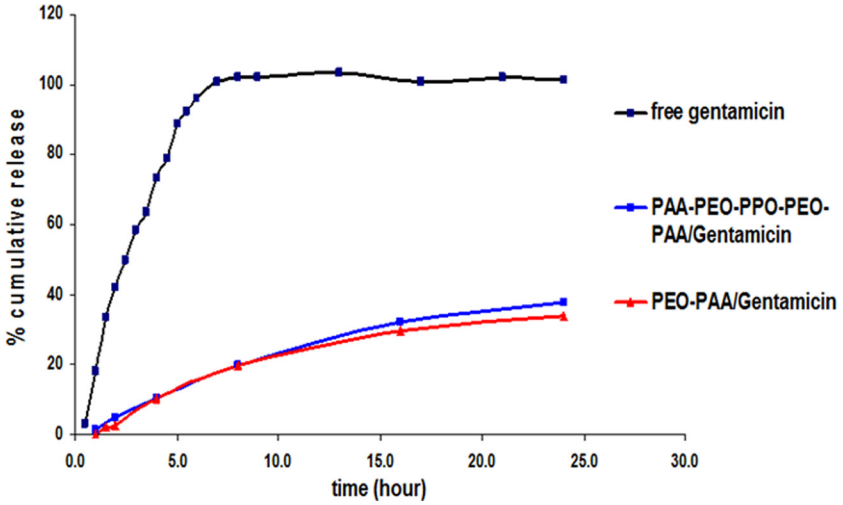

FIG. 3. Drug-releasing characteristics of the nanostructures at pH 7.4 and 37°C.

REFERENCES

1. **Batrakova, E., S. Lee, S. Li, A. Venne, V. Alakhov, and A. Kabanov.** 1999. Fundamental relationships between the composition of pluronic block copolymers and their hypersensitization effect in MDR cancer cells. Pharm. Res. **16:**1373–1379.
2. **Batrakova, E. V., S. Li, Y. Li, V. Y. Alakhov, W. F. Elmquist, and A. V. Kabanov.** 2004. Distribution kinetics of a micelle-forming block copolymer Pluronic P85. J. Control. Release **100:**389–397.
3. **Durante-Mangoni, E., A. Grammatikos, R. Utili, and M. E. Falagas.** 2009. Do we still need the aminoglycosides? Int. J. Antimicrob. Agents **33:**201–205.
4. **Fattal, E., J. Rojas, M. Youssef, P. Couvreur, and A. Andremont.** 1991. Liposome-entrapped ampicillin in the treatment of experimental murine listeriosis and salmonellosis. Antimicrob. Agents Chemother. **35:**770–772.
5. **Lecaroz, C., C. Gamazo, and M. J. Blanco-Prieto.** 2006. Nanocarriers with gentamicin to treat intracellular pathogens. J. Nanosci. Nanotechnol. **6:** 3296–3302.
6. **Lecaroz, C., C. Gamazo, M. J. Renedo, and M. J. Blanco-Prieto.** 2006. Biodegradable micro- and nanoparticles as long-term delivery vehicles for gentamicin. J. Microencapsul. **23:**782–792.
7. **Lutwyche, P., C. Cordeiro, D. J. Wiseman, M. St. Louis, M. Uh, M. J. Hope, M. S. Webb, and B. B. Finlay.** 1998. Intracellular delivery and antibacterial activity of gentamicin encapsulated in pH-sensitive liposomes. Antimicrob. Agents Chemother. **42:**2511–2520.
8. **Prior, S., B. Gander, J. M. Irache, and C. Gamazo.** 2005. Gentamicin-loaded microspheres for treatment of experimental Brucella abortus infection in mice. J. Antimicrob. Chemother. **55:**1032–1036.
9. **Ranjan, A., P. N., M. Seleem, J. Jain, N. Sriranganathan, J. S. Riffle, and R. Kasimanickam.** 2009. Drug delivery using novel nanoplexes against a Salmonella mouse infection model. J. Nanopart. Res. doi:10.1007/s11051-009-9641-y.
10. **Raybourne, R. B., and V. K. Bunning.** 1994. Bacterium-host cell interactions at the cellular level: fluorescent labeling of bacteria and analysis of short-term bacterium-phagocyte interaction by flow cytometry. Infect. Immun. **62:**665–672.
11. **Ristuccia, A. M., and B. A. Cunha.** 1982. The aminoglycosides. Med. Clin. N. Am. **66:**303–312.
12. **Sano, G., Y. Takada, S. Goto, K. Maruyama, Y. Shindo, K. Oka, H. Matsui, and K. Matsuo.** 2007. Flagella facilitate escape of Salmonella from oncotic macrophages. J. Bacteriol. **189:**8224–8232.
13. **Seleem, M. N., M. Ali, S. M. Boyle, and N. Sriranganathan.** 2008. Vectors for enhanced gene expression and protein purification in Salmonella. Gene **421:**95–98.
14. **Seleem, M. N., N. Jain, N. Pothayee, A. Ranjan, J. S. Riffle, and N. Sriranganathan.** 2009. Targeting Brucella melitensis with polymeric nanoparticles containing streptomycin and doxycycline. FEMS Microbiol. Lett. **294:**24–31.
15. **Tian, Y., L. Bromberg, S. N. Lin, T. A. Hatton, and K. C. Tam.** 2007. Complexation and release of doxorubicin from its complexes with pluronic P85-b-poly(acrylic acid) block copolymers. J. Control. Release. **121:**137–145.